OMTN, Volume *27*

Supplemental information

Analysis of the circRNA and T-UCR populations identifies convergent pathways in mouse and human models of Rett syndrome

Edilene Siqueira, Aida Obiols-Guardia, Olga C. Jorge-Torres, Cristina Oliveira-Mateos, Marta Soler, Deepthi Ramesh-Kumar, Fernando Setién, Daniëlle van Rossum, Ainhoa Pascual-Alonso, Clara Xiol, Cristina Ivan, Masayoshi Shimizu, Judith Armstrong, George A. Calin, R. Jeroen Pasterkamp, Manel Esteller, and Sonia Guil

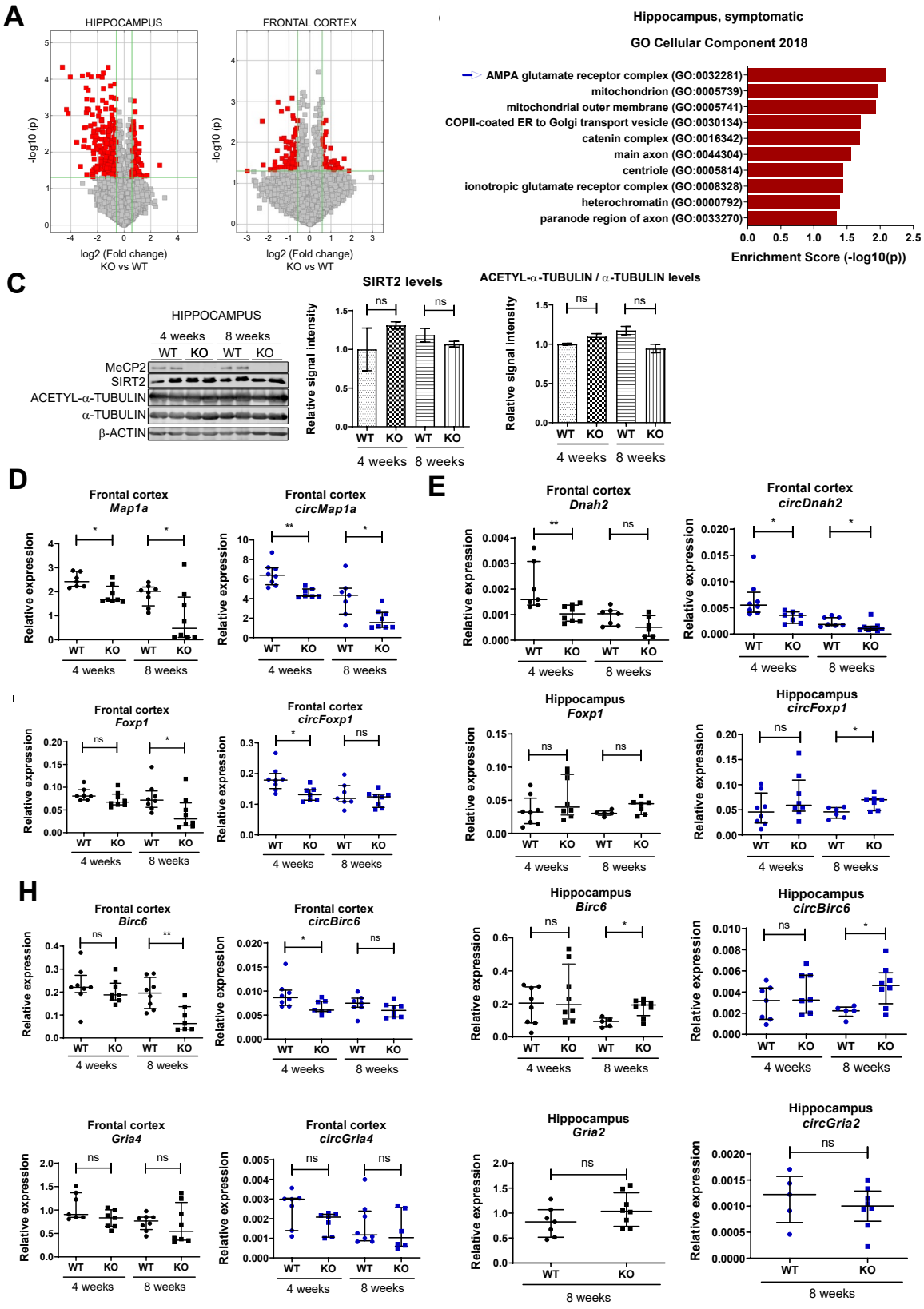

Figure S1. Related to Figure 1. Characterization of circular RNA species in *Mecp2*-KO mice. (A) Volcano plots for visualizing differential expression between WT and *Mecp2*-KO samples in hippocampus and frontal cortex of symptomatic mice. The vertical lines correspond to 1.5-fold greater and lesser values, and the horizontal line represents $p < 0.05$ (two-tailed unpaired t test).

Each red point on the plot represents significantly differentially expressed circRNAs. (B) Enriched Gene Ontology terms (Cellular Component 2018) for the host genes of altered circRNA (> 2-FC), as identified by functional clustering (Enrichr). (C) Western blot analysis of MeCP2, SIRT2, acetyl-α-TUBULIN and α-TUBULIN in the hippocampus from WT and KO pre-symptomatic and symptomatic mice. Samples from two animals per condition are shown. Graphs on the right represent quantitation of band intensity (two-tailed unpaired t test, ns = not significant). (D)-(K) Expression levels of host linear and circular species were analyzed by RT-qPCR in the indicated brain regions of WT and *Mecp2*-KO pre-symptomatic (4-week-old) and symptomatic (8-week-old) mice. Graphs represent the median and interquartile range of 6-8 replicates from different animals per condition (two-tailed Mann-Whitney U test, ** $p < 0.01$, * $p < 0.05$, ns = not significant).

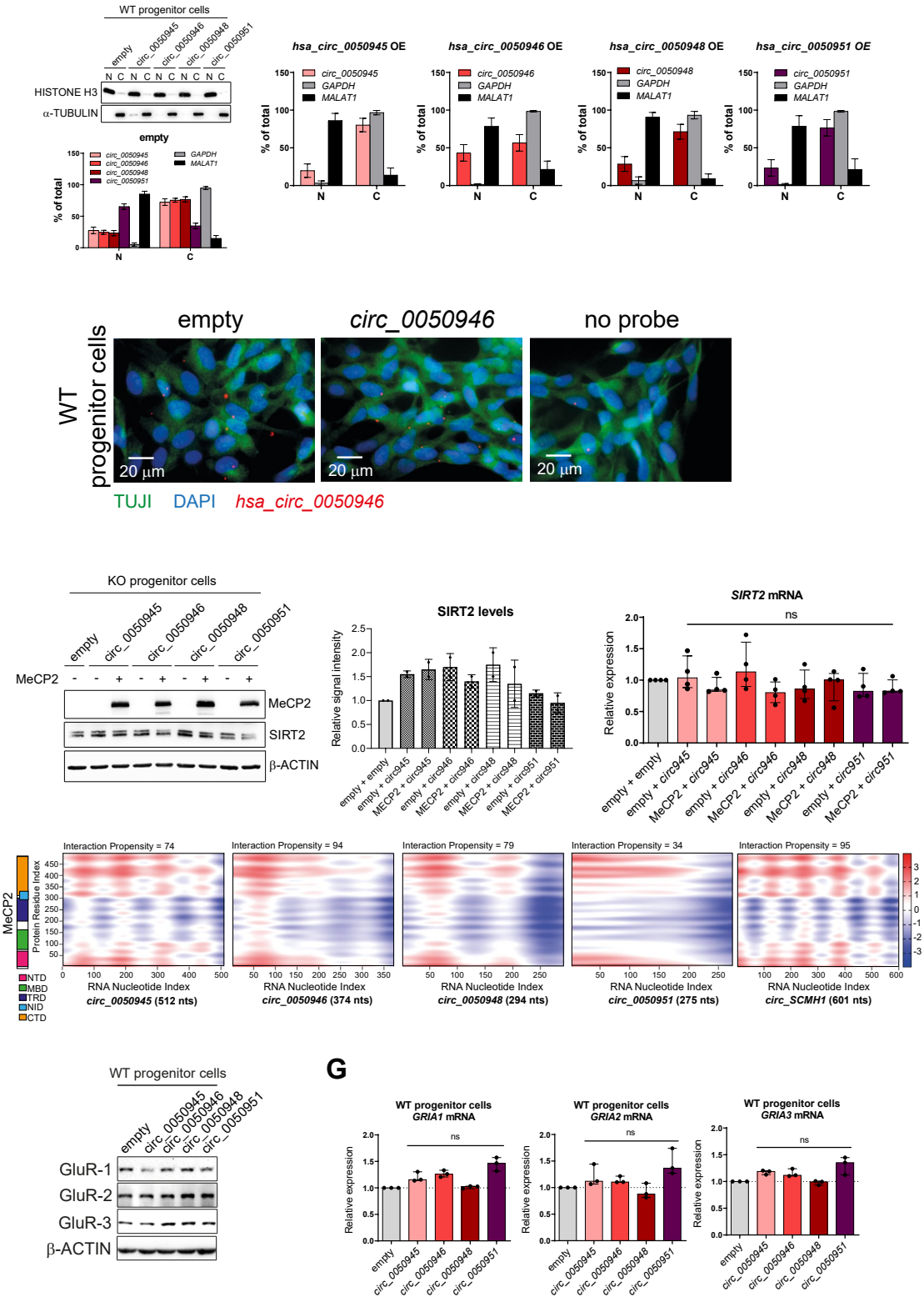

Figure S2. Related to Figure 2. Characterization of circRNAs derived from human *SIRT2* locus. (**A**) Nuclear/cytoplasmic fractionation of WT neural progenitor cells (control or overexpressing (OE) specific circRNAs, as indicated), analyzed by RT-qPCR and western blot to assess fraction purity. *GAPDH* and *MALAT1* are used as references of cytoplasmic and nuclear RNAs, respectively. (**B**) RNA ISH showing localization of overexpressed human *hsa_circ_0050946* in WT neural progenitor cells. Colocalization with the neuronal marker TUJ1 is shown. (**C**) Western blot analysis of MeCP2 and SIRT2 in *MeCP2*-KO progenitor cells upon

overexpression of the different *circSIRT2* and/or MeCP2, as indicated. The graph on the right represents quantitation of band intensity of two representative experiments. (**D**) Expression levels of *SIRT2* mRNA was analyzed by RT-qPCR in the same samples as in (C). The graph shows the median and interquartile range (one-way ANOVA, ns = not significant). (**E**) Prediction of *circSIRT2s*-MeCP2 interactions by using the catRAPID algorithm. Prediction for *circSCMH1* is also shown for comparison. (**F**). Western blot analysis of GluR receptor subunits in WT progenitor cells upon overexpression of the indicated *circSIRT2s*. (**G**) Expression levels of *GRIA1/2/3* mRNA was analyzed by RT-qPCR in the same samples as in (E). The graph shows the median and interquartile range (one-way ANOVA, ns = not significant).

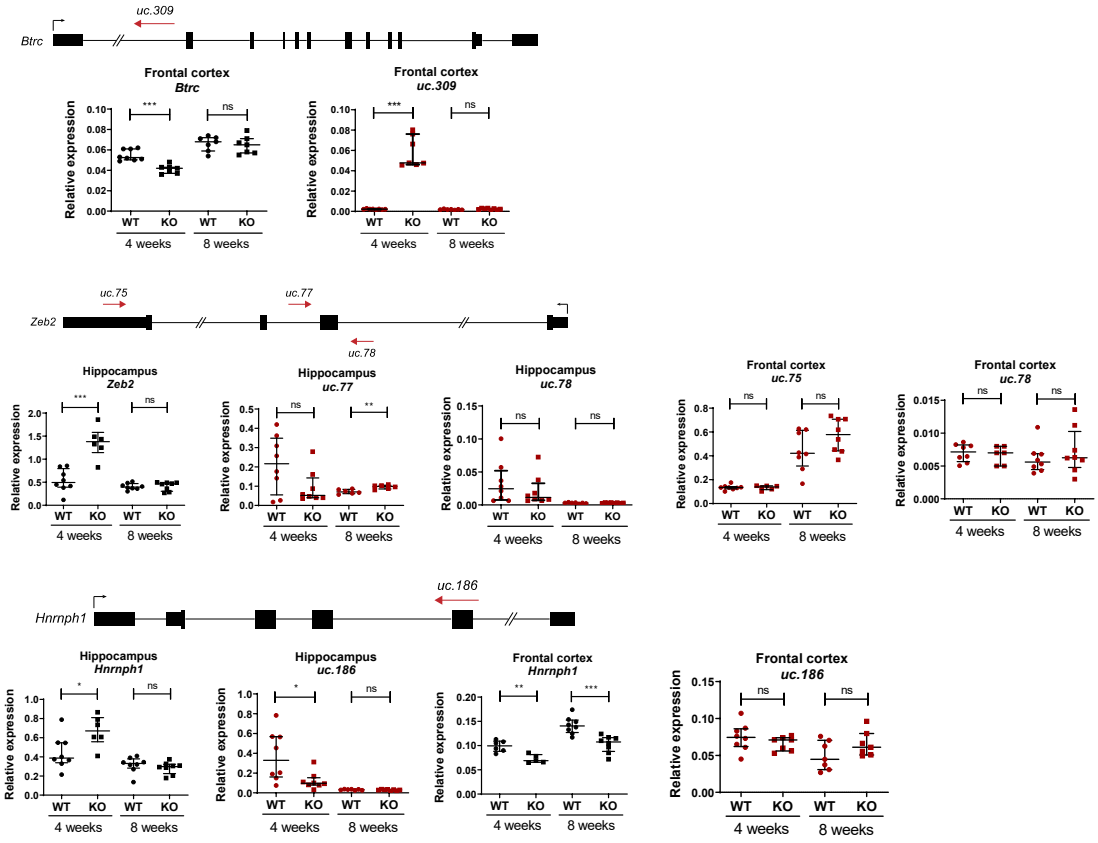

Figure S3. Related to Figure 4. Validation of T-UCR expression in *Mecp2*-KO mice. (**A**)-(**C**) RT-qPCR analysis and validation of candidate altered T-UCRs and their corresponding host genes in the indicated brain regions from WT and KO pre-symptomatic (4-week-old) and symptomatic mice (8-week-old). Diagrams represent genomic organization of each locus, and location and sense of T-UCR transcription are indicated by the red arrows. Graphs represent the median with interquartile range of 6-8 replicates from different animals per condition (two-tailed Mann-Whitney U test, * $p < 0.05$, ** $p < 0.01$, *** $p < 0.001$, ns = not significant).

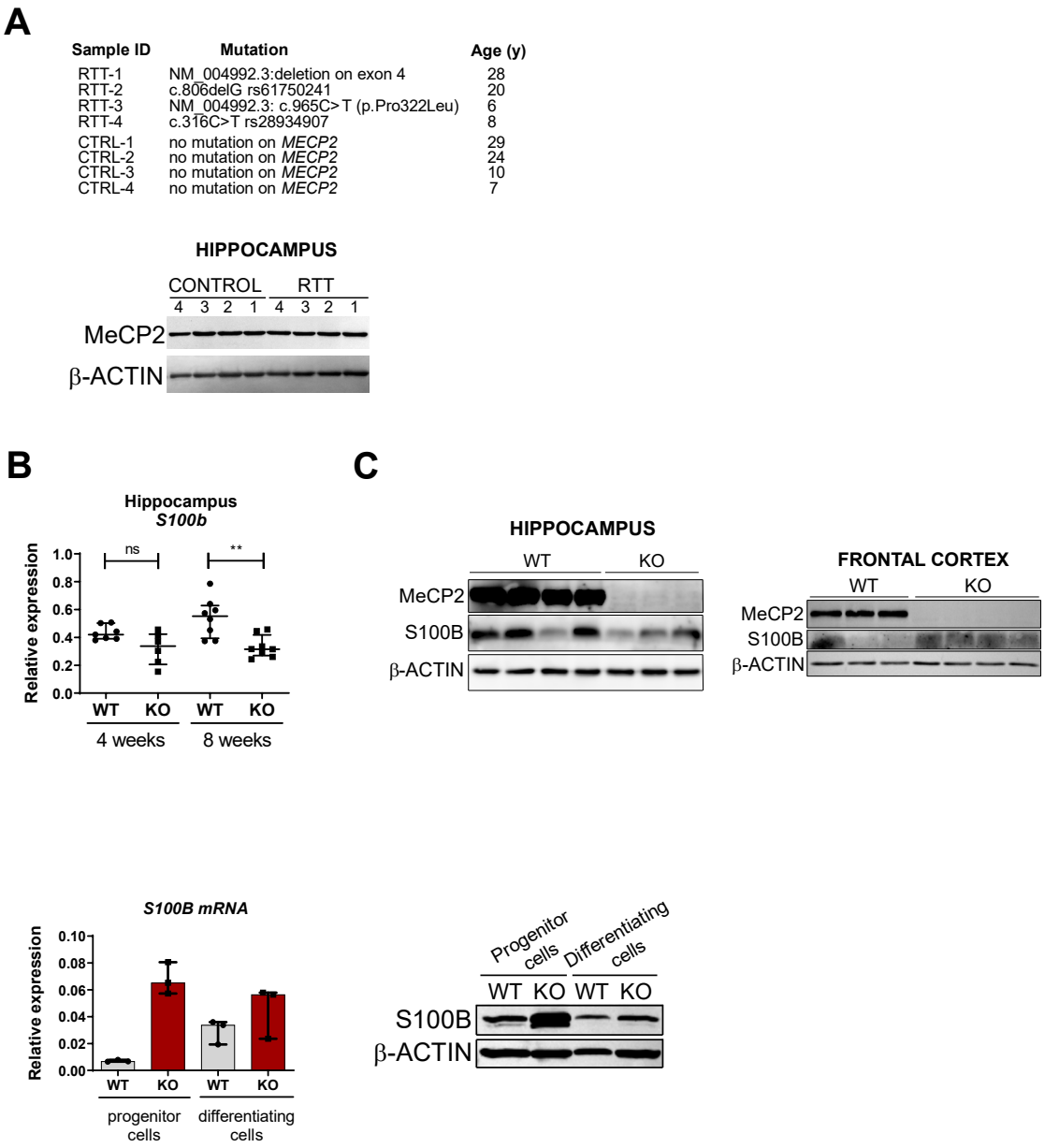

Figure S4. Related to Figure 4. S100B levels in different models of RTT. (A) *Upper list*, Genotype of post-mortem samples used in this study (4 control and 4 RTT patients). The mutation type found on MeCP2 for each RTT patient, as well as the age, is indicated. Below, western blot analysis of MeCP2 levels in the same samples. (B) Total RNA from the hippocampus of WT and *Mecp2*-KO pre-symptomatic (4-week-old) and symptomatic mice (8-week-old) was analyzed by RT-qPCR to assess *S100b* transcript levels. Graphs represent the median and interquartile range of 6-8 independent animals. Two-tailed Mann-Whitney U test were used (** $p < 0.01$, ns = not significant). (C) Western blot analysis of MeCP2 and S100B in the hippocampus from WT and *Mecp2*-KO symptomatic mice. Samples from 3-4 animals per condition are shown. (D) Western blot analysis of MeCP2 and S100B in the frontal cortex from WT and *Mecp2*-KO symptomatic mice. Samples from 3-4 animals per condition are shown. (E) S100B levels in WT or *MeCP2*-KO neural progenitor or differentiating cells (30 days) were analyzed by RT-qPCR. Graphs represent the median and interquartile range of three independent replicates. (F) Western blot analysis of S100B in WT and *MeCP2-KO* neural progenitor or differentiating cells (30 days).

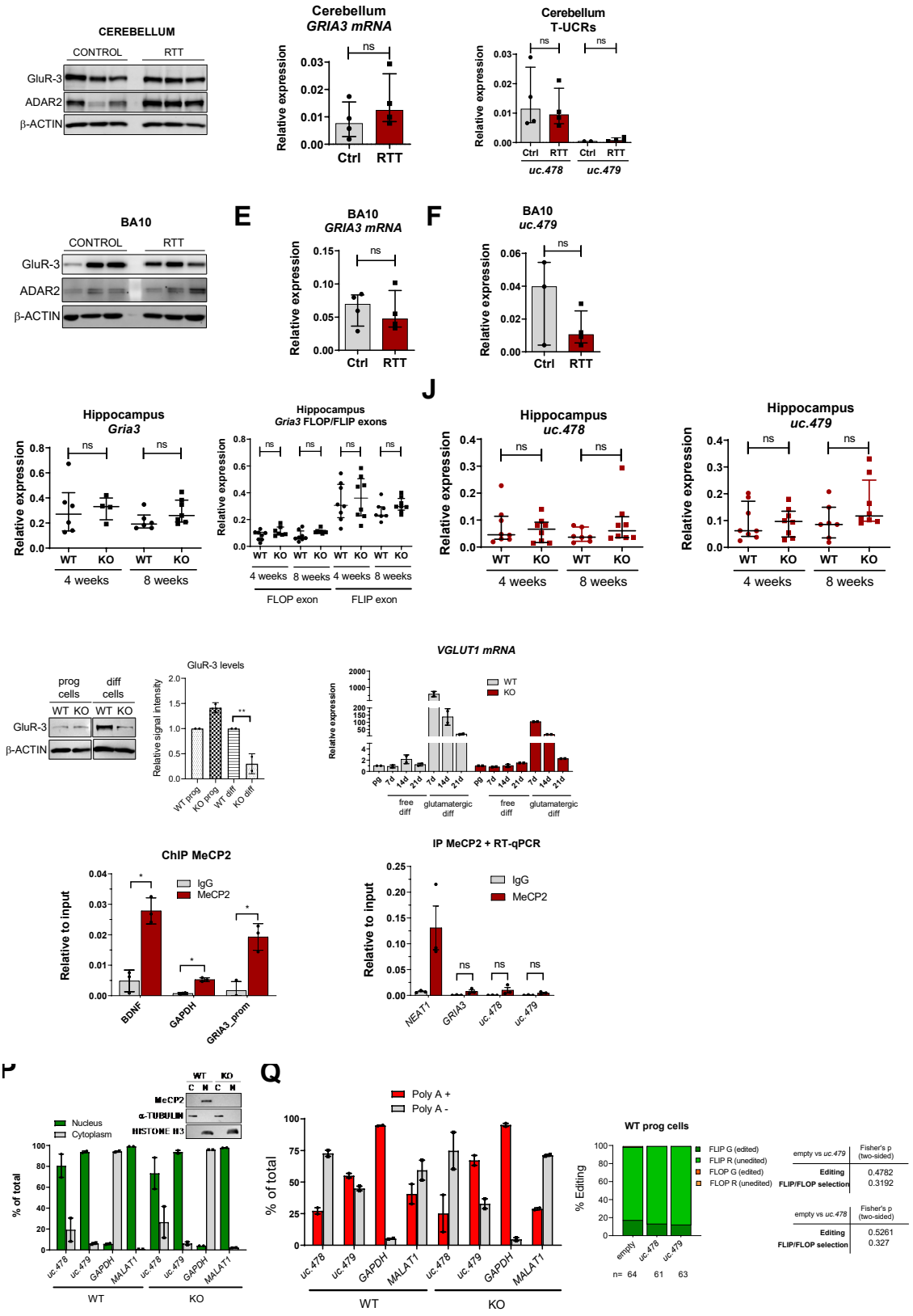

Figure S5. Related to Figure 5. Analysis of *GRIA3* locus expression. (**A**) Western blot analysis of GluR-3 and ADAR2 in the cerebellum of three post-mortem RTT patients and three healthy control's samples. (**B**) and (**C**) Expression levels of *GRIA3* mRNA and the T-UCRs *uc.478* and

uc.479 were analyzed in the same samples as in (A) by RT-qPCR. Graphs represent the median with interquartile range of the data from the three subjects per group (two-tailed Mann–Whitney U test, ns = not significant). (**D**) Western blot analysis of GluR-3 and ADAR2 in the Brodmann area 10 (BA10) of three post-mortem RTT patients and three healthy control samples. (**E**) and (**F**) Expression levels of *GRIA3* mRNA and the T-UCRs *uc.478* and *uc.479* were analyzed in the same samples as in (D) by RT-qPCR. Graphs represent the median with interquartile range of the data from the three subjects per group (two-tailed Mann–Whitney U test, ns = not significant,). (**G**) Methylation analysis of DNA from post-mortem control or RTT hippocampus. The regions surrounding the alternative exons flop and flip on the *GRIA3* gene (including location of T-UCRs) are depicted, and all CpGs are marked with an asterisk. Graphs represent the average percentage of methylation of three replicates ± SD for each position. For each replicate, at least 20 clones were sequenced. (**H**)-(**K**) Expression levels of *Gria3*, alternatively spliced exons flip and flop, *uc.478 and uc.479*, were analyzed by RT-qPCR in the hippocampus of WT, or *Mecp2*-KO pre-symptomatic (4-week-old) and symptomatic (8-week-old) mice. Graphs show the median and interquartile range of six to eight replicates from different animals per condition (two-tailed Mann–Whitney U test, ns = not significant). (**L**) Western blot analysis of GluR-3 in WT or KO cells (progenitor (prog) or upon glutamatergic differentiation (diff)). The graphs on the right represent quantitation of band intensity of two representative experiments (one-way ANOVA test was used, ** $p < 0.01$). (**M**) Expression levels of *VGLUT1* (marker of glutamatergic differentiation) were analyzed by RT-qPCR along the time-course of differentiation. (**N**) Chromatin immunoprecipitation (ChIP) coupled to qPCR to determine MeCP2 binding to *GRIA3* promoter in WT progenitor cells. The graph represents the mean ± SD of three independent experiments. The enrichments corresponding to *BDNF* and *GAPDH* promoters are shown for comparison. Two-tailed Mann-Whitney U test were used (* $p < 0.05$, ns = not significant). (**O**) RT-qPCR analysis of retrieved RNA following MeCP2 immunoprecipitation in WT progenitor cells. *GRIA3* locus-derived transcripts were analyzed. *NEAT1* was used as positive control. Graph represents the mean ± SEM of at least 3 independent experiments. Two-tailed Mann-Whitney U test was used (ns = not significant). (**P**) Nuclear/cytoplasmic fractionation of WT or KO neural progenitor cells were analyzed by RT-qPCR and western blot to assess fraction purity. *GAPDH* and *MALAT-1* are used as references of cytoplasmic and nuclear RNAs, respectively. (**Q**) Poly(A)+/poly(A)- partition of total RNA from WT and KO neural progenitor cells and analysis by RT-qPCR. *GAPDH* and *MALAT1* are used as references of poly(A)+ and poly(A)- RNAs, respectively. Graphs represent the means ±SD of 2 replicates of poly(A) selection. (**R**) Analysis of editing and alternative splicing choice of *GRIA3* mRNA in WT neural progenitor cells overexpressed with *uc.478* or *uc.479*. Percentages correspond to pooled data from sequences of at least two replicates per condition. The contingency graph displays flip/flop selection and the associated edited/unedited status. Fisher's exact test (two-tailed) was used to estimate the statistical significance of the editing and alternative splicing analyses.

Table S1. Oligos used in this work.

Name	Sequence 5' - 3'	Experiment	Species
Mecp2 exon1 Fw	CAATTGACGGCATCGCCGCTGAGA	*MeCP2* genotyping	Human
Mecp2 exon1 Rv	CATCCGCCAGCCGTGTCGTCCGAC	*MeCP2* genotyping	Human
Mecp2 exon2 Fw	CACTGTGTGTTACGTGCCAGT	*MeCP2* genotyping	Human
Mecp2 exon2 Rv	GGCACAGTTTGGCACAGTTAT	*MeCP2* genotyping	Human
Mecp2 exon3 Fw	TCTCTGTTGTCCTGGGGAAG	*MeCP2* genotyping	Human
Mecp2 exon3 Rv	CCCTGGGCACATACATTTTC	*MeCP2* genotyping	Human
Mecp2 exon4a Fw	GGCAGTGTGACTCTCGTTCA	*MeCP2* genotyping	Human
Mecp2 exon4a Rv	AGTCCTTTCCCGCTCTTCTC	*MeCP2* genotyping	Human
Mecp2 exon4b Fw	GAGACCGTACTCCCCATCAA	*MeCP2* genotyping	Human
Mecp2 exon4b Rv	CCAACTACTCCCACCCTGAA	*MeCP2* genotyping	Human
sgRNA MECP2_1 Fw	CACCGGATTTTGACTTCACGGTAAC	CRISPR sgRNA	Mouse
sgRNA MECP2_1 Rv	AAACGTTACCGTGAAGTCAAAATCC	CRISPR sgRNA	Mouse
sgRNA MECP2_2 Fw	CACCGGGCGCTCCATTATCCGTGAC	CRISPR sgRNA	Mouse
sgRNA MECP2_2 Rv	AAACGTCACGGATAATGGAGCGCCC	CRISPR sgRNA	Mouse
BsGria3 Flop_reg1 Fw	TGGTGTTTTTGTTATTTTTTTTT	Methylation analysis	Human
BsGria3 Flop_reg1 Rv	TTTATCCAAAAAACCTTACTCA	Methylation analysis	Human
BsGria3 Flop_reg2 Fw	TAAGGTTTTTTGGATAAATTGA	Methylation analysis	Human
BsGria3 Flop_reg2 Rv	AAAAATAACCTAATCATTCCACTT	Methylation analysis	Human
BsGria3 Flip_reg0 Fw	ATTTGTTTTTTGTTTGGAAGTA	Methylation analysis	Human
BsGria3 Flip_reg0 Rv	AAACCCTAACCACAAAATAATT	Methylation analysis	Human
BsGria3 Flip_reg1 Fw	AAGGTAATGTTTAGGTTGTTTGTA	Methylation analysis	Human
BsGria3 Flip_reg1 Rv	CTAAAATACCTTATTCACTAAATTTCA	Methylation analysis	Human
BsGria3 Flip_reg2 Fw	ATAAGTTGAAAAATAAATGGTGG	Methylation analysis	Human
BsGria3 Flip_reg2 Rv	AACCAAATTAAATTTCCTAATCA	Methylation analysis	Human
uc.478-BamHI Fw	CTGGGATCCTTTTTATACGTTAACGATTTCC	Cloning	Human
uc.478-EcoRI Rv	ttttttttGAATTCTAATAAGATAACAGTCTTGCC	Cloning	Human
uc.479-BamHI Fw	CTGGGATCCTTAACTTTTTATAAGGTAATGCTCAGG	Cloning	Human

uc.479-EcoRI Rv	ttttttttGAATTCACAAAAAGACCTTCAGCGA	Cloning	Human
hsa_circ_0050945-BstEII Fw	TCGATTGGTAACCCTCCTCACCCCTCTTCCCTCCATCTCTCCCTCTAGAacatagataccctggagcg	Cloning	Human
hsa_circ_0050945-SacII Rv	TCGATTCCGCGGGGCTCAGGACAGGCTGGGGTTGCTCAGCTCCTCACcttccatccaaggagctc	Cloning	Human
hsa_circ_0050946-SacII Rv	TCGATTCCGCGGCCTGTGACGACGGGGGCTTGAAGAAGGGCTCTTACctggccagctttctccttg	Cloning	Human
hsa_circ_0050948-SacII Rv	TCGATTCCGCGGCTTGCTGATGAGGGAGGCAAAGGGCTGCACctgcaaggaggtacccatg	Cloning	Human
hsa_circ_0050951-BstEII Fw	TCGATTGGTAACCCGGTGTCATATGGTGCATAAGTTCCTCTCCTCCAGGtcgcagagtcatctgtttg	Cloning	Human
hsa_circ_0050951-SacII Rv	TCGATTCCGCGGCCCATCCTCCTCCCAGGATGCTCGCATCCGCCTACctgcgtgtagcagcgcagg	Cloning	Human
hMeCP2-ex4 Fw	GTGTATTTGATCAATCCCCAGGGAAAAGCCTTTCGCTCTAAAGTGGAG	Cloning	Human
hMeCP2-ex3 Rv	CTTTTCCCTGGGGATTGATCAAATACACATCATACTTCCCAGCAGAGCGGC	Cloning	Human
hMeCP2e1-Fus-EcoRI Fw	ttttttttGAATTCGCCGCCACCATGGCTGCTGCTGCTGCTGCTCCTTCTGGAGGAGGAGGAGGAGGAGAAGAAGAAAGAC	Cloning	Human
hMeCP2e1-Fus Fw	GGAGGAGGAGAAGAAGAAAGACTGGAAGAAAAGTCAGAAGACCAGGACCTC	Cloning	Human
mmu_circ_41253-EcoRV Fw	TCGATTGATATCaaaccttagcatgtgccatcaatcctctgttccagGccgcaaggtcatctgtttg	Cloning	Mouse
mmu_circ_41253-BstEII Rv	TCGATTGGTAACCTACCCATGGTCACACCTGCCCGTGGCCCCGCCTACctgcgtgtagcagcgcagc	Cloning	Mouse
mMeCP2-EcoRI Fw	ttttttttGAATTCGCCGCCACCATGGCCGCCCGCTGCCGCCACCGCCGC	Cloning	Mouse
hMeCP2-BamHI Rv	ttttttttGGATCCTCAGCTAACTCTCTCGGTCACGGGCGTCCGGCTGTC	Cloning	Mouse and Human
GRIA1 Fw	AGGTGCCAATTTCCCCAACA	RT-qPCR	Human
GRIA1 Rv	AGCAGCATGTTCCTGTGACT	RT-qPCR	Human
GRIA2 Fw	TTCAGATGAGACCCGACCTC	RT-qPCR	Human
GRIA2 Rv	GCACAGCTTGCAGTGTTGAT	RT-qPCR	Human
GRIA3 Fw	TCACTACATGCTCGCTAACCT	RT-qPCR	Human
GRIA3 Rv	CCATGCATGACTCTTTCCAG	RT-qPCR	Human
SIRT2 Fw	TTGCTGAGCTCCTTGGATGG	RT-qPCR	Human
SIRT2 Rv	CTCGTCCTTGGCAGGTGGCG	RT-qPCR	Human
hsa_circ_0050945 Fw	TGGATGGAAGAACATAGATACCC	RT-qPCR	Human
hsa_circ_0050945 Rv	GCTGACGCAGTGTGATGTGT	RT-qPCR	Human
hsa_circ_0050946 Fw	GCTGGCCAGAACATAGATACC	RT-qPCR	Human
hsa_circ_0050946 Rv	GCTGACGCAGTGTGATGTGT	RT-qPCR	Human
hsa_circ_0050948 Fw	CTCCTTGCAGAACATAGATACC	RT-qPCR	Human
hsa_circ_0050948 Rv	GCTGACGCAGTGTGATGTGT	RT-qPCR	Human
hsa_circ_0050951 Fw	CTACACGCAGGTCGCAGA	RT-qPCR	Human
hsa_circ_0050951 Rv	GTCATAGAGGCCGGTGGATG	RT-qPCR	Human
vGlut1 Fw	CAGCCAACAGAGTTTTCGGC	RT-qPCR	Human
vGlut1 Rv	CGACTCCGTTCTAAGGGTGG	RT-qPCR	Human

vGlut2 Fw	TTGTGGTGGTTTTGGCATGG	RT-qPCR	Human
vGlut2 Rv	ACTGGCATATCTTGGAGCGA	RT-qPCR	Human
L13 Fw	CGGACCGTGCGAGGTAT	RT-qPCR	Human
L13 Rv	CACCATCCGCTTTTTCTTGTC	RT-qPCR	Human
B2m Fw	CATGGCTCGCTCGGTGACC	RT-qPCR	Mouse
B2m Rv	AATGTGAGGCGGGTGGAACTG	RT-qPCR	Mouse
SIRT2 Fw	GCACTGGGCCCTCTTAACAT	RT-qPCR	Mouse
SIRT2 Rv	CTGGGATTGAGTTGGGGACC	RT-qPCR	Mouse
circSirt2 Fw	CCAACCATCTGCCACTACTTC	RT-qPCR	Mouse
circSirt2 Rv	CCCACCAAACAGATGACCTT	RT-qPCR	Mouse
Map1a Fw	TAGAACCCGAGGGAGACCTT	RT-qPCR	Mouse
Map1a Rv	GCAGGAAACAGTGAGGAAGG	RT-qPCR	Mouse
circMap1a Fw	TATCAAAACTTCGCCCAGGT	RT-qPCR	Mouse
circMap1a Rv	ATGGTGAACCTCTGAGCTGA	RT-qPCR	Mouse
Dnah2 Fw	CTTGCGGACCTGCACTCCTA	RT-qPCR	Mouse
Dnah2 Rv	GAGTCTCCAGGTTGGGTAGGT	RT-qPCR	Mouse
circDnah2 Fw	CTCATCTCAGACCTGCGGAATC	RT-qPCR	Mouse
circDnah2 Rv	CGCATTGTTAGTCATGCCAC	RT-qPCR	Mouse
Foxp1 Fw	CAGTCTTGTGGCGTTCTGC	RT-qPCR	Mouse
Foxp1 Rv	CGTCTCACCCCTGAGCTTTTA	RT-qPCR	Mouse
circFoxp1 Fw	GTGAGACGTGACCTTTGGAG	RT-qPCR	Mouse
circFoxp1 Rv	GCCATAAAAAGCCTGGGGTC	RT-qPCR	Mouse
Birc6 Fw	CAGGATGGGACGTGGAACAA	RT-qPCR	Mouse
Birc6 Rv	CCCATTGACAGCACCACTCA	RT-qPCR	Mouse
circBirc6 Fw	TTCTGGAGCTCCTCAGTCAGT	RT-qPCR	Mouse
circBirc6 Rv	CCTGCGGCGGAGTCGTT	RT-qPCR	Mouse
Gria4 Fw	AAAAGCACAGGACCTCGAAA	RT-qPCR	Mouse
Gria4 Rv	TGCTGTGTCATTGCCAAGAG	RT-qPCR	Mouse
circGria4 Fw	TTCAAGGACTGACTGGGAATG	RT-qPCR	Mouse
circGria4 Rv	GTAGCCTTTGACGTGCTTCC	RT-qPCR	Mouse
Gria2 Fw	CCATCGAAAGTGCTGAGGAT	RT-qPCR	Mouse
Gria2 Rv	AGGGCTCTGCACTCCTCATA	RT-qPCR	Mouse
circGria2 Fw	CCATCGAAAGTGCTGAGGAT	RT-qPCR	Mouse
circGria2 Rv	CTCCTGCATTTCCTCTCCTG	RT-qPCR	Mouse
Btrc Fw	CCAGGCTTTGCATAAACCAA	RT-qPCR	Mouse
Btrc Rv	CACAATCATGCTGGAAGTGC	RT-qPCR	Mouse
Hnrnph1 Fw	CGGCTTAGAGGACTCCCTTT	RT-qPCR	Mouse
Hnrnph1 Rv	TATCCCATTTGGCACGATTT	RT-qPCR	Mouse
Zeb2 Fw	CCAATCCCAGGAGGAAAAAC	RT-qPCR	Mouse
Zeb2 Rv	GAGGGTTTGCAAGGCTATCA	RT-qPCR	Mouse
Gli3 Fw	CCTTCCATCCTCCTGTACCA	RT-qPCR	Mouse
Gli3 Rv	TCTGGATACGTCGGGCTACT	RT-qPCR	Mouse
Meis2 Fw	GATGACGACGATCCAGACAA	RT-qPCR	Mouse
Meis2 Rv	TCTGAAGGGTACGGGTGTGT	RT-qPCR	Mouse
S100b Fw	GGTGACAAGCACAAGCTGAA	RT-qPCR	Mouse
S100b Rv	GTCCAGCGTCTCCATCACTT	RT-qPCR	Mouse
Gria3 flop Fw	AGCAGAGAAAGCCGTGTGAT	RT-qPCR	Mouse
Gria3 flop Rv	AAGAGGCCTTGCTCATTCAG	RT-qPCR	Mouse
Gria3 flip Fw	AGCAGAGAAAGCCGTGTGAT	RT-qPCR	Mouse
Gria3 flip Rv	GAGTCCTTGGCTCCACATTC	RT-qPCR	Mouse
uc.75 Fw	AAATTGAAAAATCCCATCTCACA	RT-qPCR	Mouse and Human
uc.75 Rv	TCATTTGGGCAAATTTTACG	RT-qPCR	Mouse and Human
uc.77 Fw	CTGTCACACTGCTCCCAAGA	RT-qPCR	Mouse and Human
uc.77 Rv	TCAGCCAAAGATGCTTGAAA	RT-qPCR	Mouse and Human

uc.78 Fw	TTGAAGGTGGCTGTTTCTGA	RT-qPCR	Mouse and Human
uc.78 Rv	GAGCTAATGCCCCGTGTTTA	RT-qPCR	Mouse and Human
uc.186 Fw	TATCCCATTTGGCACGATTT	RT-qPCR	Mouse and Human
uc.186 Rv	TCATTTCTGGGCTTGTGATG	RT-qPCR	Mouse and Human
uc.220 Fw	AATTGCCTCCTTCCAGAAAGT	RT-qPCR	Mouse and Human
uc.220 Rv	CCCAAGTAAAAGTGCCTTCG	RT-qPCR	Mouse and Human
uc.221 Fw	CCCCAGGATCAATTCTGAAC	RT-qPCR	Mouse and Human
uc.221 Rv	CAGCGGGCTACATGAAAAAT	RT-qPCR	Mouse and Human
uc.309 Fw	GCTCATTTCTGGCAGGTTTT	RT-qPCR	Mouse and Human
uc.309 Rv	GAACTTGATCGATGGCTGCT	RT-qPCR	Mouse and Human
uc.478 Fw	AAGCATTTGTGCATTTTCTTACAA	RT-qPCR	Mouse and Human
uc.478 Rv	AAGAGGCCTTGCTCATTCAG	RT-qPCR	Mouse and Human
uc.479 Fw	CCCCTGCTTTATCGCTTTCT	RT-qPCR	Mouse and Human
uc.479 Rv	CGTTCTTCACGTGGGAAATAA	RT-qPCR	Mouse and Human
GRIA3 Fw	GGATTCCAAAGGCTATGGTG	Editing and splicing analysis	Human
GRIA3 Rv	ATAGAAAACGCCTGCCACAT	Editing and splicing analysis	Human
Gria3 Fw	AGCAGAGAAAGCCGTGTGAT	Editing and splicing analysis	Mouse
Gria3 Rv	CTGCCCGTGATTTGTAACAG	Editing and splicing analysis	Mouse
GAPDH Fw	TCTTCTTTTGCGTCGCCAG	RT-qPCR N/C fractioning	Human
GAPDH Rv	AGCCCCAGCCTTCTCCA	RT-qPCR N/C fractioning	Human
MALAT1 Fw	AAGGTCAAGAGAAGTGTCAGC	RT-qPCR N/C fractioning	Human
MALAT1 Rv	AATGTTAAGAGAAGCCCAGGG	RT-qPCR N/C fractioning	Human
GAPDH Fw	AGGTGAAGGTCGGAGTCAA	ChIP	Human
GAPDH Rv	CCCATACGACTGCAAAGACC	ChIP	Human
BDNF Fw	CTGGTAATTCGTGCACTAGAGT	ChIP	Human
BDNF Rv	CACGAGAGGGCTCCACGGT	ChIP	Human
SIRT2prom Fw	CCCCAGTTAGGTAAGAAAGCG	ChIP	Human
SIRT2prom Rv	CCAATCAGAGTATTCGGGAGG	ChIP	Human
GRIA3prom Fw	GAAAGGAAGAGTGAGCGAGAG	ChIP	Human
GRIA3prom Rv	GCCTAAAACGAAGCTGACAAG	ChIP	Human
NEAT1 Fw	TTCCTCCTTCCACACAGACC	IP RT-qPCR	Human

NEAT1 Rv	GAAGGAAGCTTGGCAAGGAG	IP RT-qPCR	Human
circSCMH1 Fw	CCACCTCTTGGATTTCGGCT	IP RT-qPCR	Human
circSCMH1 Rv	AGTGACAAGCACCTCTGAGC	IP RT-qPCR	Human